Study of liquid metals as a basis for nanoscience

2008 J. Phys.: Condens. Matter 20 114101

(http://iopscience.iop.org/0953-8984/20/11/114101)

IOP PUBLISHING JOURNAL OF PHYSICS: CONDENSED MATTER

J. Phys.: Condens. Matter **20** (2008) 114101 (6pp) doi:10.1088/0953-8984/20/11/114101

Study of liquid metals as a basis for nanoscience

Makoto Yao and Yoshinori Ohmasa

Department of Physics, Graduate School of Science, Kyoto University, 606-8502 Kyoto, Japan

E-mail: yao@scphys.kyoto-u.ac.jp

Received 30 August 2007
Published 20 February 2008
Online at stacks.iop.org/JPhysCM/20/114101

Abstract

There are two ways to proceed with nanoscience: so-called top-down and bottom-up methods. Usually, the former methods are thought of as in the province of physicists and the latter in that of chemists. However, this is not entirely true because the physics of disordered matter, especially liquid metals, is well-developed bottom-up science and it has indeed provided nanoscience with basic ideas and theoretical tools such as *ab initio* molecular dynamics (MD) simulations.

Here we wish to present experimental studies on such phenomena that originate from quantum mechanical properties and subsequently lead to classical non-equilibrium processes: among these are slow dynamics due to metal–nonmetal transitions in liquids, and wetting and dewetting transitions of liquid semiconductors. Since all these phenomena are related to a spatiotemporal range far wider than that treated by the present *ab initio* MD simulations, it is desirable that new progress in theoretical physics be stimulated, resulting in further developments in nanoscience.

1. Introduction

It is widely accepted that the notions of nanoscience and nanotechnology were first suggested in a celebrated lecture by Feynman in 1959 [1]. Since then, the notions have spread from physics to chemistry, engineering, medicine and pharmacy [2]. One might think that such developments have nothing to do with studies of liquid metals, but there *is* a close relation between nanoscience and the physics of disordered matter: the Bloch theorem cannot be applied to either system. This is why basic ideas and theoretical tools developed in the fields of liquid metals, which are represented by *ab initio* molecular dynamics (MD) simulations, have been applied to nanostructured materials recently.

In 1985, Car and Parrinello [3] devised a new simulation method by combining a classical MD simulation with the Kohn–Sham density functional theory, and succeeded in explaining why liquid silicon is metallic in contrast to crystalline and amorphous silicon. It was at the seventh conference in the International Conferences on Liquid and Amorphous Metals (LAM) series in 1989, organized by Endo [4], that *ab initio* MD was adopted as one of the main topics for the first time. The relation between the topology of atomic arrangements and the electronic properties of liquid selenium was lectured on by Hohl [5], and the electronic states localized in molten salts by Selloni [6]. Later, *ab initio* MD was extended to study metal–nonmetal (M–NM) transitions in fluid mercury [7] and selenium [8] near the liquid–gas critical point.

The purpose of the present presentation, however, is not to give a review of theoretical or computer simulation studies, but to report such experimental results as cannot be reproduced by the present *ab initio* MD simulations. We are hoping that new progress in theoretical physics will be stimulated by these experimental works, which may result in further developments in nanoscience. For more than ten years, our research has engaged with slow dynamics and interfacial properties, which are less studied in the field of liquid metals. On the other hand, although the phase transition dynamics and the interfacial properties attract considerable interest in soft matter physics [9], they are treated only in phenomenological manners and the quantum degrees of freedom behind these phenomena are usually left untouched.

In the next section we present experimental evidence for slow dynamics due to the metal–nonmetal (M–NM) transitions, especially for liquid Se. In section 3, wetting phenomena and interface dynamics are elucidated for the liquid Se–Tl system. In section 4, we discuss the possibility of three-dimensional structural analysis by utilizing a free electron laser. All these topics are related to a spatiotemporal range far

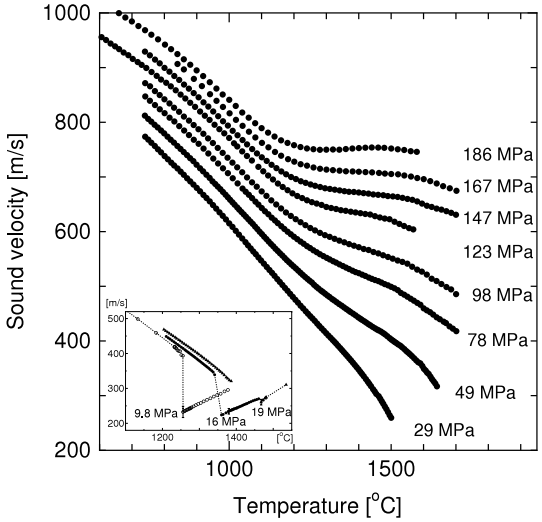

Figure 1. Sound velocity v_s in liquid Se at various pressures. The inset shows v_s near the vapour pressure curve.

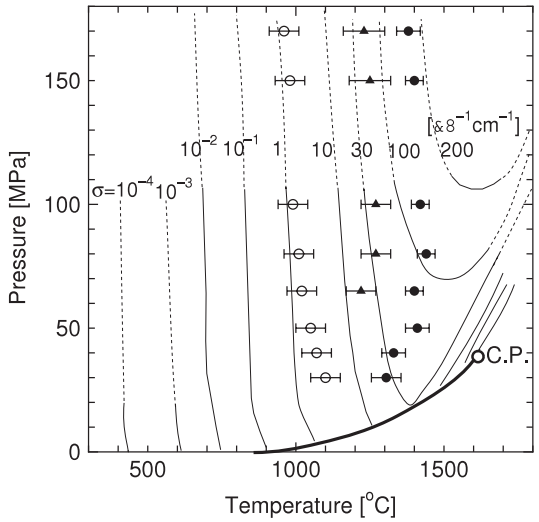

Figure 2. The state point on the P–T plane corresponding to the minimum (open circles) and maximum (closed circles) of the temperature derivative of v_s. The triangles denote the maximum of the bulk viscosity. The bold line is the vapour pressure curve, and the thin lines are conductivity contours.

wider than that treated by the present *ab initio* MD simulations. It will be stressed that liquid metals are good objects of study when one wants to bridge between quantum mechanical degrees of freedom and classical non-equilibrium processes.

2. Slow dynamics due to the metal–nonmetal transition

Near the triple point the electronic properties of most liquid metals can be described using a nearly free electron model. However, when a liquid metal is expanded by heating up near its liquid–gas critical point, the electrons tend to be strongly scattered by less-screened ions, and subsequently the metallic states are transformed to nonmetallic [10]. In particular, the M–NM transition in expanded liquid Hg has been well studied since the late 1960s, because its critical temperature is the lowest among the metallic elements, and it is widely accepted that the M–NM transition can be attributed to a lack of overlapping between the 6s and 6p bands [7, 11].

However, the dynamic aspect of the M–NM transition was not studied until Kohno and Yao [12] observed anomalously large sound attenuation at supercritical pressures and proposed slow structural relaxation with a timescale of 2 ns. Subsequently, Kobayashi *et al* [13] found discontinuities in the temperature and pressure coefficients of the adiabatic sound velocity at subcritical pressures. Interestingly, the adiabatic sound velocity exhibits a density dependence opposite to that of the microscopic sound velocity which Ishikawa *et al* [14] deduced from inelastic x-ray scattering (IXS). The microscopic sound velocity remains large on the metallic side, and it decreases rapidly on the nonmetallic side, suggesting that the microscopic sound is rather sensitive to the electronic properties. In other words, the adiabatic sound should be interpreted as a result of many stochastic processes that may reflect density fluctuations in the M–NM transition region. Furthermore, Inui *et al* [15] observed anomalous behaviours in x-ray small angle scattering not only in the liquid–gas critical region but also in the M–NM transition region. Analysing these scattering data by using the Ornstein–Zernike formula, they have attributed the anomaly in the M–NM transition region to the second moment of the direct correlation function, in contrast to the critical anomaly which is generally attributed to the total correlation function.

Our group has extended ultrasonic measurements to other liquid systems that undergo a M–NM transition. In what follows, we restrict ourselves to the semiconductor–metal (S–M) transition in liquid selenium [16] and Se–Te mixtures. Near the melting point, liquid Se has twofold chain structure and shows semiconducting properties. As the temperature increases, the chain molecules are progressively broken, and consequently lead to dimers in the liquid–gas supercritical region ($T_c = 1615\,^\circ$C, $P_c = 38.5$ MPa), where fluid Se becomes an insulator [17]. These behaviours are common to sulfur, but a clear distinction between Se and S is that the former is easily transformed to a metal under high pressure [18].

Figure 1 shows the adiabatic sound velocity v_s of liquid and gaseous Se as a function of temperature [16, 19]. The measurements were carried out at constant pressures by utilizing a phase-sensitive method. At low pressures v_s decreases monotonically with increasing temperature, while at pressures higher than 180 MPa the v_s–T curve has an S-like shape with a minimum and a maximum, which is similar to that for liquid Se–Te mixtures [20, 21]. Since the relative experimental error in v_s is less than 0.2%, we can safely take its temperature derivative $(\partial v_s/\partial T)_P$, from which the temperature of the minimum and maximum of $(\partial v_s/\partial T)_P$ can be estimated within an error of $\pm 50\,^\circ$C.

In figure 2 the minimum temperatures T_{min} are denoted by open circles, and the maximum temperatures T_{max} by closed circles on the temperature and pressure (T–P) plane. It should be noted that T_{min} nearly coincides with the conductivity

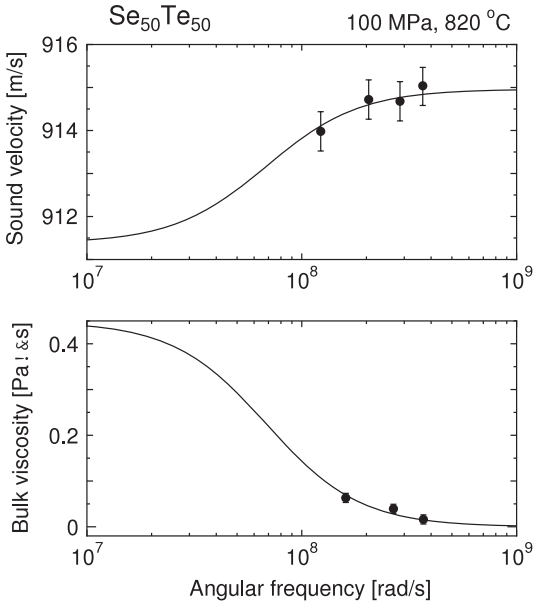

Figure 3. Frequency dependence of v_s (upper panel) and bulk viscosity (lower panel) for a liquid $Se_{50}Te_{50}$ mixture. The lines are the fitting curves drawn by assuming Debye-type relaxation.

contour of 1 $\Omega^{-1}\,cm^{-1}$ and that T_{max} appears when the conductivity is between 100 and 200 $\Omega^{-1}\,cm^{-1}$, that is, near the minimum metallic conductivity, except at low pressures where the critical phenomena are not ignored. These results indicate that the electronic properties of liquid Se deeply influence the sound velocity.

We have also measured the sound absorption for liquid Se. It is known that the sound absorption of liquid is, in general, composed of three terms: the shear viscosity η term, the bulk viscosity ζ term and the thermal conductivity κ term. Since η and κ are negligibly small in the S–M transition region of liquid Se, the observed absorption can be attributed to large ζ. The maximum of the sound absorption appears along the conductivity contour of 30 $\Omega^{-1}\,cm^{-1}$, i.e. at the mid-point of the S–M transition, as shown by the triangles in figure 2 [16]. It is interesting that the slow dynamics is common to Hg and Se, though there are considerable differences in atomic arrangement and M–NM transition mechanism between them.

The S–M transition temperature can be lowered by adding tellurium to liquid Se. For liquid Se–Te mixtures we have estimated the relaxation time τ by measuring the frequency dependence of the sound velocity [21] and sound absorption [22, 23]. The results are displayed in figure 3. Assuming a single Debye relaxation process, we have estimated such a τ that reproduces the sound dispersion (see the upper panel of figure 3) and the frequency dependence of ζ (see the lower panel) simultaneously, and it is determined as 15 ± 3 ns. To elucidate the spatiotemporal correlation of the slow dynamics, we have carried out neutron spin echo experiments for a liquid Se–Te mixture [24]. The results are consistent with the relaxation time estimated from the ultrasonic measurements.

There are several open questions for the slow dynamics in the M–NM transition region. Is the slow dynamics due to the M–NM transition universal like that in the vicinity of the liquid–gas critical point? Is the slow dynamics a precursor of a first-order phase transition [13]? A general and the most important question may be 'How can we build a bridge between a microscopic picture relating to the quantum mechanical processes (in this case, the M–NM transition) and a macroscopic picture relating to the classical non-equilibrium processes (in this case, slow dynamics)?'

3. Wetting phenomena and interface dynamics

Wetting is a macroscopic phenomenon but the wettability (ability of wetting) is controlled by microscopic interactions. Wetting is a kind of three-phase-coexistence phenomenon, and the degree of wetting is described by a contact angle defined by the three phases [25]. The relation between the contact angle and the interfacial tensions is given by the Young equation. In 1977, Cahn [26] studied the asymptotic behaviour of the Young equation on approaching the liquid–gas critical point, and predicted the necessity of wetting near the critical point (i.e. the critical-point wetting). Several experimental observations of critical-point wetting were reported in the field of liquid metals in the late 1990s [27].

Recently, we have found unusual wetting behaviour in liquid selenium–thallium mixtures contacting a silica wall [28]. First of all, the system does not show the critical-point wetting near the liquid–liquid critical point. The phase diagram of the Se–Tl mixture on the Se-rich side is displayed in figure 4(a), where the critical concentration is 7.95 at.% Se and the critical temperature is 454 °C [29]. In contrast, when the temperature goes down from the critical temperature, a Se-rich wetting film intrudes between the Tl-rich bulk liquid and the silica wall. Furthermore, the wetting film disappears when the silica wall is slightly heated relative to the bulk liquid sample. Figure 4(b) shows a wetting phase diagram, where the abscissa is the internal temperature T_I of the bulk liquid sample, and the ordinate is the temperature difference ΔT between the wall temperature T_W and T_I. Below the phase boundary, the Se-rich wetting film covers the Tl-rich bulk liquid, while it disappears at high ΔT or in the high T_I region. The apparent absence of the critical-point wetting can be qualitatively explained by taking the combined effects of the gravity and a long-range interaction [28] into account. It should be emphasized that the long-range interaction is closely related to the highly polarizable nature of a Se–Tl mixture which undergoes a S–M transition with increasing Tl concentration.

A more interesting observation is that transient wetting appears when there is a small temperature drop of the non-wetting states [30]. Examples of the starting and ending temperatures are depicted in figure 4(b). A time evolution of the wetting behaviour starting from $T_I = 300\,°C$ is illustrated in figure 5. Immediately after the temperature drop, a Se-rich wetting film spreads over the Tl-rich bulk phase, leading to a complete wetting at a time τ_1 (i.e. wetting time). The complete wetting persists for a time τ_2 (i.e. the persistence time), and then it takes a time τ_3 (i.e. the dewetting time) for the Se-rich film to withdraw from the lower part of the sample cell. The time evolution was recorded at various temperatures, and

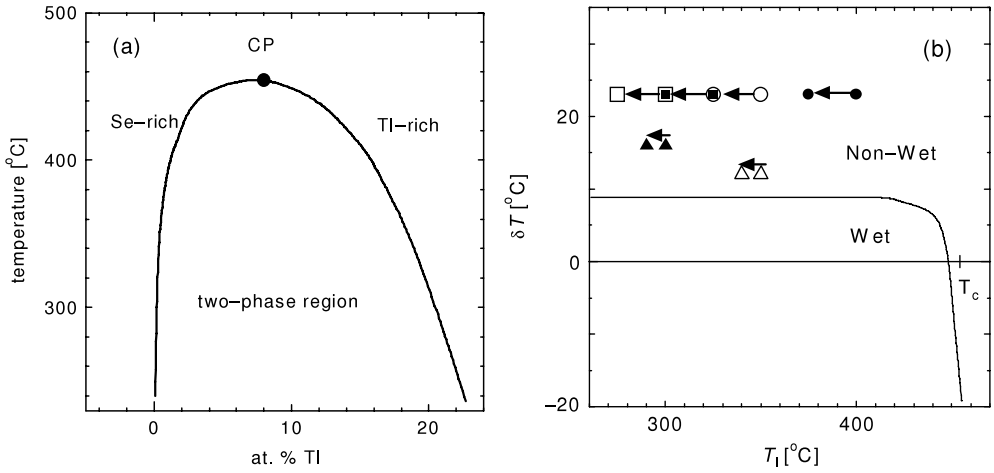

Figure 4. (a) Phase diagram of a liquid Se–Tl binary mixture on the concentration and temperature plane [29]. (b) Wetting phase diagram on the plane of the internal temperature T_I and the surface temperature δT relative to T_I. The symbols with arrows denote the initial and final temperatures for each quench.

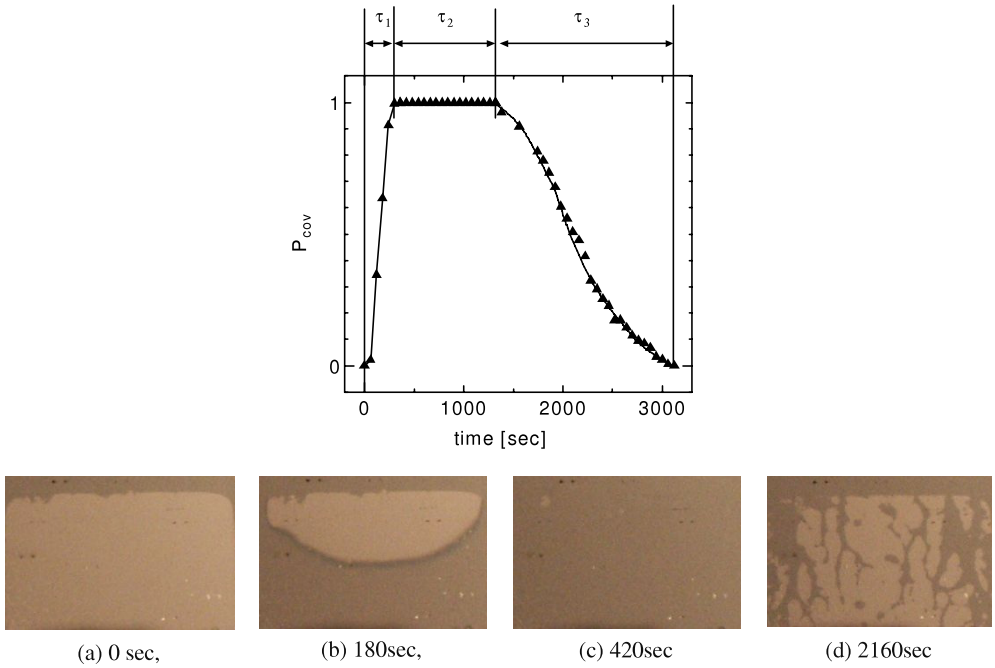

Figure 5. Time evolution of the wetting behaviour starting from $T_I = 300\,^{\circ}\mathrm{C}$ for a liquid Se–Tl mixture contacting a quartz wall. Lower panels: (a) non-wetting, (b) wetting, (c) complete wetting, and (d) dewetting. Upper panel: fraction of Se-rich wetting layer. τ_1 is the wetting time, τ_2 the persistence time, and τ_3 the dewetting time.

it proved that both τ_2 and τ_3 have Arrhenius-type temperature dependence with an activation energy very close to that of the viscosity, indicating that the dewetting process can be classified as a viscosity dewetting [31]. However, a precise analysis of the fraction of non-wetting area (i.e. dry patches) [30] reveals that the dewetting process of the Se–Tl mixture is decelerated compared with the ideal viscosity dewetting process in which the fraction of dry patches increases in proportion to the square of time [31].

Since the dewetting processes may be regarded as interface dynamics, we have performed a naive experiment on the liquid–liquid interface [32]. It is known that the thermopower of the liquid Se–Tl mixture changes its sign from negative to positive when the amount of Tl exceeds the critical concentration [33]. This implies that, when a Se–Tl mixture with the critical concentration is separated into two liquid–liquid phases, a p–n junction could be formed automatically. Here p stands for a p-type semiconductor and n for an n-type semiconductor. Then we measured the I–V characteristics (here I being the current, V the generated voltage), though the expected rectification effect was not observed at all. This implies that the electric double layer which causes the rectification effect at the crystalline p–n junction does not exist in the liquid state.

However, unusual relaxation processes were found when the direction of current was reversed. The relaxation process

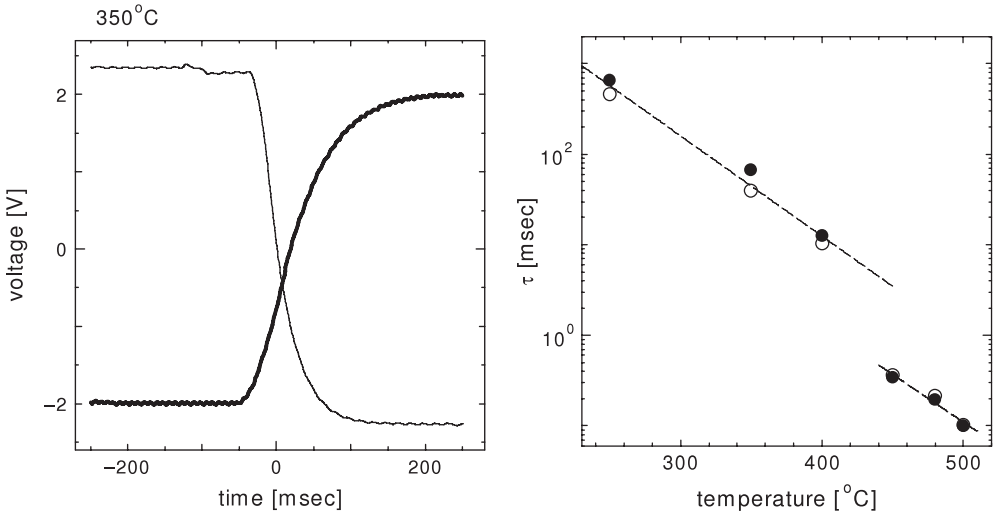

Figure 6. Left: time evolution of the voltage generated between the two electrodes, one in the Se-rich upper part and the other in the Tl-rich lower part, after the direction of the current is changed from normal (i.e. Tl-rich → Se-rich case) to reverse (thin line), and from reverse to normal (bold line). Right: temperature dependence of the relaxation time for the normal to reverse case (open circles) and that for the reverse to normal case (closed circle). The former is lesser than the latter below the critical temperature T_c, while no appreciable difference is seen above T_c. The lines are guides for the eye.

can be described using a single exponential, and the relaxation time $\tau_{n\to r}$ after the switching from the normal current to the reverse current is shorter than the time $\tau_{r\to n}$ for switching from the reverse to the normal current, as seen in figure 6(a). Figure 6(b) shows the temperature dependences of $\tau_{n\to r}$ and $\tau_{r\to n}$. At the lowest temperature, both $\tau_{n\to r}$ and $\tau_{r\to n}$ are very long (nearly 1 s), and decrease rapidly with increasing temperature. Above the critical temperature, both $\tau_{n\to r}$ and $\tau_{r\to n}$ become shorter and the difference between them vanishes. These results suggest that the ultraslow relaxation should be associated with the liquid–liquid interface. It is concluded that, although the p–n junction does not exist in the equilibrium liquid, a remnant of the p–n junction could appear temporarily after the switching, because the spatial distribution of ions changes very slowly compared with the rearrangement of electrons and holes.

As regards the ultraslow interface dynamics and the deceleration of the dewetting process, it may be instructive to refer to theoretical works by Onuki and his group [34, 35]. They have studied the interfacial structure and the interface dynamics of immiscible mixtures of polar and nonpolar liquids containing hydrophilic ions and hydrophobic counter-ions. Solving the Cahn–Hilliard equation coupled with the Poisson equation, they have found that a slight addition of the ions substantially slows down the interface dynamics. The hydrophilic ions are favoured by the polar liquid and the hydrophobic ions by the nonpolar liquid. Since, in our case, the electrons are favoured by the Se-rich liquid and the holes by the Tl-rich liquid, an analogy could be drawn with the polar–nonpolar mixtures.

4. Three-dimensional structural analysis by utilizing a free electron laser

Although x-ray diffraction provides the most popular and most powerful method of structural analysis, only one-dimensional (1D) information is available for disordered materials as long as laboratory x-ray and conventional synchrotron radiations are used. However, if one uses a coherent x-ray source, two-dimensional (2D) structural information can be obtained. Since an x-ray free electron laser (XFEL) is now being planned for Japan, Europe and the United States, the possibility of three-dimensional (3D) structural analysis using XFEL is briefly discussed in this section.

The expected intensity of XFEL is so strong that just one shot of XFEL is sufficient for recording a 2D diffraction pattern. However, the exposure to very intense x-rays will result in the Coulomb explosion of the specimen [36]. Therefore, the duration of the x-ray pulse must be of the order of femtoseconds, because otherwise the diffraction pattern would inevitably include the signals from the exploded sample. Moreover, since the microscopic structure is always changing in the liquid state, true 3D analysis could be feasible only if many diffraction patterns from various incidence angles could be simultaneously recorded.

Therefore, the second best solution may be to take 2D patterns, as many as possible, and construct a real-space image by using phase-retrieval methods [37, 38] or reverse Monte Carlo (RMC) simulations [39]. In contrast to the conventional RMC approach, where 3D information is deduced from a single 1D pattern, the RMC approach combined with XFEL use should have far greater reliability because, in this case, a great number of 2D diffraction patterns can be used as raw data.

In a suggested experimental set-up a very small amount of liquid specimen would be injected through a tiny nozzle in coincidence with an x-ray pulse. It should be noted that this method is essentially the same as the free cluster experiment. We are now constructing a new cluster apparatus that can be used for XFEL experiments as well as the detection technique. Recently, a multiple-ion coincidence momentum imaging technique [40] has been developed and applied to

study the Coulomb explosion of clusters for the first time [41]. Finally, it may be instructive to point out that the Coulomb explosion is triggered by a quantum mechanical process and leads to a non-equilibrium phenomenon, which is, in a sense, common to the slow dynamics due to the M–NM transition and the wetting dynamics.

5. Summary

Conventionally, the atomic arrangements and the electronic properties consistent with the microscopic structure have been the major objects of study in the liquid metal field, and their understanding has been substantially improved through the invention of new theoretical techniques such *ab initio* MD simulations. Here, however, we have concentrated upon such experimental results as cannot be reproduced by the present *ab initio* MD simulations, hoping that new progress in theoretical physics will be stimulated. A brief explanation of 3D structural analysis using XFEL is also given.

Acknowledgments

The authors are grateful to Dr H Kajikawa, Mr K Fujii, Mr S Takahashi, Professors K Maruyama and H Endo for collaboration in this work, and to Professor A Onuki and Mr A Minami for valuable discussions about the charge effects on the liquid–liquid interface. This work was partially supported by the Grant-in-Aid for Scientific Research 'Non-equilibrium soft matter physics' from the MEXT of Japan, the Grant-in-Aid for the 21st Century COE 'Center for Diversity and Universality in Physics' from the MEXT of Japan, and the Grant-in-Aid for the 'Promotion of X-ray Free Electron Laser Research' from the MEXT of Japan.

References

[1] Feynman R P *There's Plenty of Room at the Bottom* e.g. http://www.zyvex.com/nanotech/feynman.html
[2] e.g. Yao M and Nagaya K (ed) 2006 *Abstract booklet of the 4th Annual Mtg of the Society of Nano Science and Technology (Kyoto, 2006)*
[3] Car R and Parrinello M 1985 *Phys. Rev. Lett.* **55** 2471
[4] Endo H (ed) 1990 *Proc. 7th Int. Conf. on Liquid and Amorphous Metals*; *J. Non-Cryst. Solids* **117/118** 915–33
[5] Hohl D and Jones R O 1990 *J. Non-Cryst. Solids* **117/118** 922
[6] Xu L F, Selloni A and Parrinello M 1990 *J. Non-Cryst. Solids* **117/118** 926
[7] Kresse G and Hafner J 1997 *Phys. Rev.* B **11** 7539
[8] Shimojo F, Hoshino K, Watabe M and Zempo Y 1998 *J. Phys.: Condens. Matter* **10** 1199
[9] e.g. Onuki A 2002 *Phase Transition Dynamics* (Cambridge: Cambridge University Press)
[10] Hensel F and Warren W W Jr 1999 *Fluid Metals, The Liquid–Vapor Transition of Metals* (Princeton, NJ: Princeton University Press)
[11] Yao M 1994 *Z. Phys. Chem.* **184** 73
[12] Kohno H and Yao M 1999 *J. Phys.: Condens. Matter* **11** 5257
Kohno H and Yao M 2001 *J. Phys.: Condens. Matter* **13** 10293–306
[13] Kobayashi K, Kajikawa H, Hiejima Y, Hoshino T and Yao M 2007 *J. Non-Cryst. Solids* **353** 3362–5
[14] Ishikawa D, Inui M, Matsuda K, Tamura K, Tsutsui S and Baron A Q R 2004 *Phys. Rev. Lett.* **93** 097801
[15] Inui M, Matsuda K, Ishikawa D, Tamura K and Ohishi Y 2007 *Phys. Rev. Lett.* **98** 185504
[16] Kajikawa H, Takahashi S, Iwakoshi M, Hoshino T and Yao M 2007 *J. Phys. Soc. Japan* **76** 14604
[17] Hoshino H, Schumutzler R W and Hensel F 1976 *Ber. Bunsenges. Phys. Chem.* **80** 27
[18] Seyer H-P, Tamura K, Hoshino H, Endo H and Hensel F 1986 *Ber. Bunsenges. Phys. Chem.* **90** 581
Ikemoto H, Yamamoto I, Yao M and Endo H 1994 *J. Phys. Soc. Japan* **63** 1611
[19] Takahashi S 2007 *Master Thesis* Kyoto University
[20] Yao M, Suzuki K and Endo H 1980 *Solid State Commun.* **34** 187
[21] Kajikawa H, Kobayashi K, Hiejima Y, Hoshino T and Yao M 2007 *J. Non-Cryst. Solids* **353** 3358–61
[22] Yao M, Itokawa N, Kohno H, Kajihara Y and Hiejima Y 2000 *J. Phys.: Condens. Matter* **12** 7323–39
[23] Kajikawa H 2007 *Doctoral Thesis* Kyoto University
[24] Ohmasa Y, Hoshino T and Yao M 2007 *J. Phys.: Condens. Matter* **19** at press
[25] e.g. Ted Davis H 1996 *Statistical Mechanics of Phases, Interfaces, and Thin Films* (New York: Wiley)
[26] Cahn J W 1977 *J. Chem. Phys.* **66** 3667
[27] Yao M and Hensel F 1996 *J. Phys.: Condens. Matter* **8** 9547
Kozhevnikov V F, Arnold D I, Naurzakov S P and Fisher M E 1997 *Phys. Rev. Lett.* **78** 1735
Tostmann H, Nattland D and Freyland W 1996 *J. Chem. Phys.* **104** 8777
[28] Ohmasa Y, Takahashi S, Fujii K, Nishikawa Y and Yao M 2006 *J. Phys.: Condens. Matter* **18** 8449
[29] Kanda F A, Faxon R C and Keller D V 1968 *Phys. Chem. Liquids* **1** 61
[30] Ohmasa Y, Takahashi S, Fujii K, Nishikawa Y and Yao M 2006 *J. Phys. Soc. Japan* **75** 084605
[31] de Gennes P-G, Brochard-Wyart F and Quere D 2004 *Capillarity and Wetting Phenomena: Drops, Bubbles, Pearls, Waves* (New York: Springer) (Translated by A Reisinger)
[32] Fujii K, Katayama T, Ohmasa Y, Nagaya K and Yao M 2007 in preparation
[33] Cutler M *et al* 1984 *Phys. Rev.* B **29** 5694
[34] Onuki A 2006 *Phys. Rev.* E **73** 021506
Kitamura H and Onuki A 2005 *J. Chem. Phys.* **123** 124513
[35] Minami A and Onuki A 2007 private communication
[36] Neutze R, Wouts R, van der Spoel D, Weckert E and Hajdu J 2000 *Nature* **406** 752
[37] Marchesini S, He H, Chapman H N, Hau-Roege S P, Noy A, Howells M R, Weierstall U and Spence J C H 2003 *Phys. Rev.* B **68** 140101
[38] Chapman H N *et al* 2006 *Nat. Phys.* **2** 839
[39] Maruyama K and Endo H 2007 private communications
[40] Ueda K and Eland J H 2005 *J. Phys. B: At. Mol. Phys.* **38** S839
[41] Iwayama H, Nagaya K, Murakami H, Ohmasa Y and Yao M 2007 *J. Chem. Phys.* **126** 024305